ACS Macro Letters

Letter

pubs.acs.org/macroletters

Detection of Surface-Immobilized Components and Their Role in Viscoelastic Reinforcement of Rubber–Silica Nanocomposites

A. Mujtaba

Institut für Physik, Martin-Luther-Universität Halle-Wittenberg, 06099 Halle (Saale), Germany

M. Keller, S. Ilisch, and H.-J. Radusch

Zentrum für Ingenieurwissenschaften, Martin-Luther-Universität Halle-Wittenberg, 06099 Halle (Saale), Germany

M. Beiner

Fraunhofer Institut für Werkstoffmechanik IWM, Walter-Hülse-Str. 1, 06120 Halle (Saale), Germany

T. Thurn-Albrecht and K. Saalwächter*

Institut für Physik, Martin-Luther-Universität Halle-Wittenberg, 06099 Halle (Saale), Germany

ABSTRACT: Immobilized polymer fractions have been claimed to be of pivotal importance for the large mechanical reinforcement observed in nanoparticle-filled elastomers but remained elusive in actual application-relevant materials. We here isolate the additive filler network contribution to the storage modulus of industrial styrene–butadiene rubber (SBR) nanocomposites filled with silica at different frequencies and temperatures and demonstrate that it is viscoelastic in nature. We further quantify the amount of immobilized polymer using solid-state NMR and establish a correlation with the mechanical reinforcement, identifying a direct, strongly nonlinear dependence on the immobilized polymer fraction. The observation of a temperature-independent filler percolation threshold suggests that immobilized polymer fractions may not necessarily form contiguous layers around the filler particles but could only reside in highly confined regions between closely packed filler particles, where they dominate the bending modulus of aggregated particles.

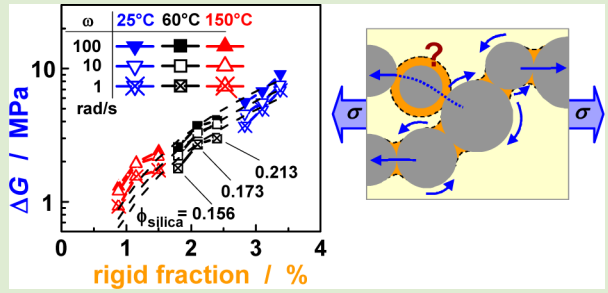

The outstanding mechanical properties of elastomer composites crucially rely on the strong synergistic effect of nanometric filler particles such as carbon black or silica and their interactions among themselves and with the elastomer matrix.[1−7] In addition to simple hydrodynamic (volumetric) arguments explaining a part of the reinforcement,[8−12] surface-immobilized fractions of the base elastomer, that play a role in connecting filler particles and likely exhibit a glass transition temperature (T_g) gradient,[13,14] have been claimed to be of pivotal importance.[2,4,7,13,15−26] While such fractions and their role in reinforcement have been confirmed for special model materials,[26] they remained elusive in actual technical reinforced elastomers. There is as of yet no consensus on their relevance for the reinforcement.[27,28]

Numerous theoretical studies[2,18,19,22] and experiments[15−17,20,23−25] have been conducted, and "glassy layers" have been either observed directly on model systems by NMR[17,25] or differential scanning calorimetry (DSC) experiments[13,21,24] or inferred indirectly for example from mechanical[15,20] or dielectric[23,24] data. In a seemingly well-established case,[15] the alleged relevance of increased-T_g material was later disproven,[28] highlighting the danger inherent to model-dependent interpretations of indirect evidence. Surface-immobilized components in technical elastomer composite materials have either not been observed directly at all or have not been directly and uniquely related to mechanical properties in the same sample. The large body of work of Montes, Lequeux, Long, and co-workers is an exception, but it is based upon an idealized model material characterized by tailored and particularly strong polymer–filler interaction.[17,25,26,29] In fact, following the finite-element simulation work of Gusev,[18] only minute amounts of increased-T_g material (down to the subpercent level) located in the gaps between or around filler particles can already explain the reinforcement effect and the additional dissipation in filled elastomers. Consequently, such small fractions may be hard to detect directly on a molecular

Received: March 31, 2014
Accepted: May 1, 2014
Published: May 8, 2014

   dx.doi.org/10.1021/mz500192r | *ACS Macro Lett.* 2014, 3, 481−485

scale by NMR, DSC, dielectric spectroscopy, or neutron scattering, suggesting a reason for the absence of corresponding signatures in previous model studies.[30]

Here, we present a combination of mechanical measurements and NMR spectroscopy and demonstrate for the first time a direct correlation between enhanced mechanical properties and quantitative immobilized-component detection in technologically relevant silica-filled styrene−butadiene rubber (SBR) samples. For details on the samples and experimental setups we refer to our previous publication.[31] We used the precipitated silica Ultrasil 7000 GR (Evonik Industries) with a surface area of 160 m^2/g and a primary particle size of around 10 nm at filler loadings of 20−80 phr (weights parts per hundred rubber parts), corresponding to silica volume fractions of ϕ_{silica} = 0.075−0.213. Our silica type, and the preparation procedure, is very similar to the one used by Baeza et al.,[32] who published an in-depth SAXS and TEM analysis of the hierarchical filler distribution and structure in very similar yet not cross-linked samples. The TEM images in Figure 1 demonstrate this similarity for the two limiting cases well below and well above the percolation threshold of the well-dispersed filler aggregates. We use shear rheology to prove the relaxatory nature of the filler-induced reinforcement effect,[31] demonstrate the separation of the filler network contribution ΔG to the plateau modulus above the percolation threshold as validated by an analysis of the samples' nonlinear response,[31] and apply proton low-field NMR for a direct molecular observation of immobilized components as a function of temperature.[13,25]

Figure 2a shows rheology data from our previous publication[31] and additional analyses, highlighting the special mechanical features of filled elastomers, such as the strong decrease of the reinforcement effect in the storage modulus with temperature[29,31] or a strong α' shoulder and significant low-frequency dissipation (LFD) in the loss modulus.[31] Notably, the shown master curves could be obtained by frequency−temperature superposition using only horizontal shift factors, a_T, with results that are nearly independent of whether G' or G'' is used as the basis of shifting. A recent study has confirmed the validity of such a treatment.[33] Figure 2b shows the same data, but using shift factors a_T from the unfilled elastomer counterpart. The inset shows this a_T (open squares) and also the one obtained for the filled elastomer (solid circles). The temperature dependence of the latter does not follow a simple Vogel−Fulcher relation but is interpreted as an apparent quantity describing a composite system with a distribution of α relaxation times with variable temperature dependence. Obviously, filled-elastomer data cannot be shifted to a master curve on the basis of just a single glass transition process;

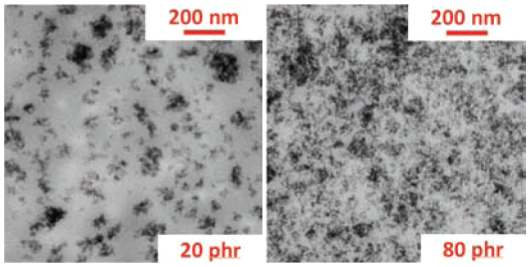

Figure 1. TEM images (slice thickness 80−100 nm, taken on a JEOL JSM 2100 at 200 kV) of the SBR samples filled with 20 and 80 phr silica, corresponding to volume fractions of 0.075 and 0.213, respectively.

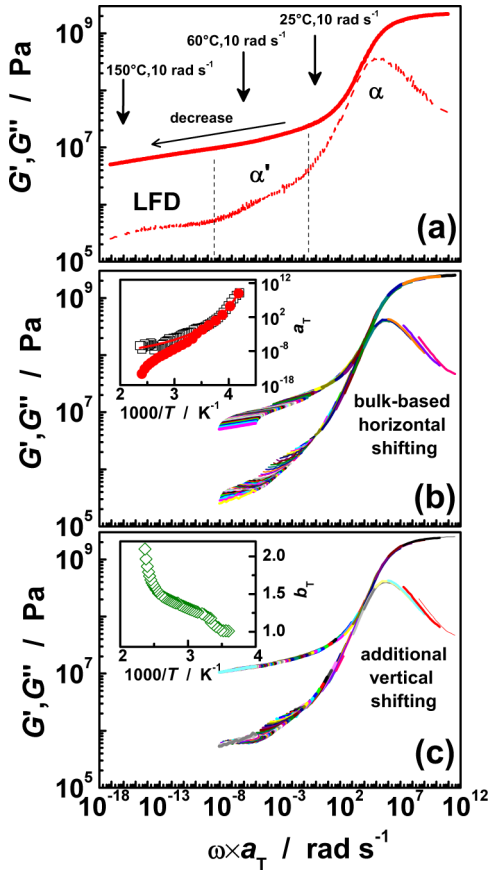

Figure 2. Master curves of storage (solid line) and loss (dashed line) moduli of an 80 phr (ϕ_{silica} = 0.213) silica-filled SBR composite, (a) after horizontal shifting with a reference temperature of 0 °C, (b) after horizontal shifting based upon shift factors of the unfilled bulk, and (c) after additional vertical shifting. The insets show (b) the horizontal shift factors of bulk (open squares) and filled SBR (filled circes) and (c) the additional vertical shift factors. The data were acquired between −35 and 150 °C with shear frequencies 0.1−100 rad/s.

however, the fact that a consistent, modified a_T can be extracted demonstrates the relaxatory, thus viscoelastic, nature of the filler-induced reinforcement.

The only known alternative to just applying a modified a_T appears to be the introduction of an independent vertical shift b_T to construct master curves also for filled elastomers.[3,20] This is demonstrated in Figure 2c, and the temperature dependence of b_T (see inset) was related to the "thermal activation of glassy-like bridges".[20] In agreement with previous work,[3] we see that both our storage and loss moduli cannot be mastered with the same vertical b_T, which was attributed to the necessarily finite strain amplitude and corresponding nonlinear effects.[20] However, mastering is possible with a single (apparent) horizontal shift factor. Due to this observation, and since b_T lacks an actual physical interpretation, we conclude that the procedure using only horizontal shifts is the more appropriate extension of the procedure usually used for unfilled polymer melts and networks.

Our mechanical data are in qualitative agreement with data of the very similar yet not cross-linked silica−SBR samples of Baeza et al.[32] These authors performed an analysis based upon a percolation model assuming additivity of purely volume-related hydrodynamic and filler network contributions. We now turn to quantifying ΔG on a similar basis, validating the

dx.doi.org/10.1021/mz500192r | ACS Macro Lett. 2014, 3, 481−485

procedure by analysis of nonlinear large-strain data as presented in our previous work,[31] which we extended to higher temperatures (150 °C) and a larger frequency range. The inset of Figure 3a shows the data analysis of nonlinear dynamic strain (γ) sweep experiments at ω = 10 rad/s, where we observe the Payne effect,[34] i.e., the reduction of the storage modulus arising from the breakdown of the percolated filler network above strains of 0.2−0.3%. The solid lines represent fits based on the Kraus model[35]

$$G'(\gamma) = G'_\infty + (G'_0 - G'_\infty)/(1 + (\gamma/\gamma_c)^{2m}) \quad (1)$$

which allows us to extract the infinite-strain limit G'_∞, where reinforcement is limited to the hydrodynamic effect of the undeformable volume taken up by the silica and occluded rubber.[31]

The limiting moduli are plotted in Figure 3a and b as a function of ϕ_{silica} for 150 and 25 °C, respectively (see ref 31 for an intermediate temperature). The difference between G'_0 and G'_∞ is particularly large above the percolation threshold ϕ_c, which, notably, is not a function of temperature. At 150 °C we see virtually no Payne effect any more below ϕ_c, while at lower temperatures effectively larger aggregates with their associated occluded rubber can still be broken down at high strain.

The values G'_∞ measured at 25 °C (and also 60 °C) are significantly above the hydrodynamic limit as predicted by the simple Einstein−Smallwood (ES) relation,[8,10] $G'_{filled} = G'_{unfilled}(1 + 2.5\phi_{filler})$ when setting $\phi_{filler} = \phi_{silica}$. Notably, the 150 °C data can be fitted in this way when adding the Guth−Gold (GG) second-order term $\sim 14.4\phi^2_{silica}$.[9] While the prefactor of 14.4 is debated and most likely too high,[12] we can nevertheless use it to fit the range $\phi_{silica} < \phi_c$ and compare it to the ES relation, using in both cases $\phi_{filler} = f\phi_{silica}$, attributing f to model inadequacies and/or occluded rubber.

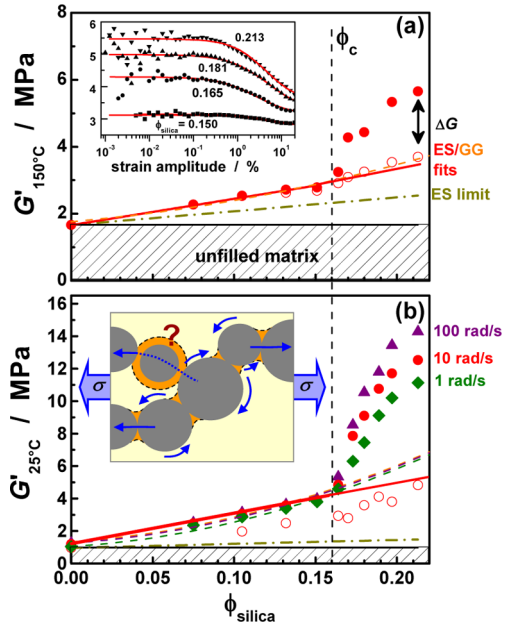

Figure 3. Storage moduli at (a) 150 °C and (b) 25 °C measured at 10 rad/s in the low-strain limit ($\gamma \to 0$, solid circles) and for $\gamma \to \infty$ (open circles). Plot (b) also includes G' data for 100 and 1 rad/s. The thick lines represent Einstein−Smallwood (ES) relations using as-prepared or scaled silica volume fractions (dash-dotted and solid lines, respectively), and the dashed lines are from Guth−Gold (GG) fits with scaled volume fractions. The diagonal hatch illustrates the limit of the plateau modulus of unfilled SBR, and the vertical dashed line indicates the constant filler percolation threshold ϕ_c. The inset in (a) shows nonlinear mechanical measurements (strain sweeps), analyzed by fits to the Kraus model, eq 1. The sketch in (b) illustrates the complex deformation modes in and near chain-like filler aggregates containing immobilized fractions in highly confined regions.

The data in Figure 3 show that below percolation the difference between the linear ES fits and the GG quadratic form is smaller than our experimental accuracy in G'_∞. For the ES fit, the factor f took values of 6, 3, and 1.8 at 25, 60, and 150 °C, respectively, while for the GG fit we obtained 2.3, 1.5 and 1.1, respectively. Values above unity reflect the amount of occluded rubber but are of course model dependent and not of central interest. An f value of 6 corresponds to an effective filler fraction above 1 for the sample with ϕ_{silica} = 0.213, which is unphysical and indicates a limitation of the ES model and that a second-order term should be included. However, as shown below, the use of either of the two limiting models leads to only minor differences in the ensuing analysis, which is based upon an extrapolation for $\phi_{silica} > \phi_c$, which do not differ much.

Importantly, the systematic increase of the f values with decreasing temperature can be attributed to the viscoelastic nature of the filler effect. Further, the observation that G' is only frequency dependent above ϕ_c (see Figure 3b), but not below, stresses this point and suggests that the viscoelastic filler network contribution is additive (note that the pure rubber matrix does not show appreciable $G'(\omega)$ dispersion in the given frequency and temperature range). Thus, in line with previous work[32] we estimated the filler network contribution ΔG to the modulus at the given temperatures and various frequencies ω as the difference between the measured G'_0 and the ES and GG extrapolations to above ϕ_c. Notably, the extrapolations provide a good fit to G'_∞ at high temperatures, while purely hydrodynamically active yet breakable agglomerates contribute at lower temperature[32] and lead to some deviations.

The inset sketch in Figure 3b highlights the complex deformation modes of the percolated filler network and provides a rationale of the temperature-independent percolation threshold. In previous work on model composites,[26] in which immobilized fractions likely form contiguous layers around spherical filler particles,[25] it was assumed that the softening of "glassy bridges" between particles separated by one or a few nanometers, as quantified by scattering results, is responsible for the Payne effect and thus the filler network modulus. This, however, should lead to a reduced percolation threshold at lower temperatures, where the particles are effectively larger. We explain the absence of such a trend with a network of closely packed filler particles that may be constituted upon processing before absorbed and equilibrated organic fractions can form.[14] It is important to note that the effective modulus of a percolated filler network is completely dominated by bending modes of the filaments.[36] This means that for the case of near-spherical (convex) filler particles a mutual "rolling off" in bending compresses or dilates possibly immobilized fractions in the interparticle gaps, explaining their relevance for the viscoelastic properties of the filler network, as addressed below.

Figure 4a shows sample data of the proton low-field NMR experiments to quantify quasirigid components, as based upon previously published procedures applied to model materials.[25,37] Our results are here, due to the rather small fractions and the limited signal-to-noise ratio, limited to detecting the most immobile signal component with a Gaussian signal shape

dx.doi.org/10.1021/mz500192r | ACS Macro Lett. 2014, 3, 481−485

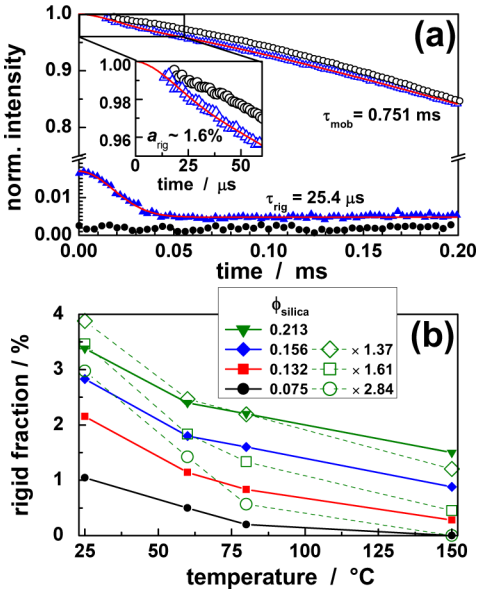

Figure 4. (a) NMR free-induction decay (FID) data of filled (ϕ_{silica} = 0.156, triangles) and pure (circles) SBR measured at 80 °C, without (open symbols) and after a short (20 μs) double-quantum filter selecting quasirigid signal components and a magic sandwich echo that overcomes the instrumental dead time (solid symbols). The latter is nonquantitative in amplitude but can be used to determine the decay time constant of the rigid fraction τ_{rig} to stabilize the fits to eq 2. The inset shows the enlarged initial FID region. (b) Signal fractions of rigid components as a function of temperature. The open symbols represent rescaled data that would always match the data from the highest silica content (solid triangles) if the immobilized fraction was strictly proportional to the silica volume fraction.

and a characteristic short decay time constant τ_{rig}. This latter quantity can be reliably determined by fits to a so-called double-quantum filtered signal in which mobile components are largely (yet not completely) suppressed (see the solid symbols in Figure 4a). The unfiltered signal is then fitted to

$$\frac{M(t)}{M_0} = a_{rig}\exp\{-(t/\tau_{rig})^2\} + (1 - a_{rig})\exp\{-(t/\tau_{mob})^b\} \quad (2)$$

with fixed τ_{rig}. In the given temperature range, its values were between 22 and 29 μs, which originates from strong dipole−dipole couplings between the spins and is representative of organic components, i.e., the SBR polymer or the silanization agent, with α relaxation times above about 10 μs, i.e., of fractions whose effective T_g is at most 40 K below the given temperature.[25] Motions which are much faster than the average inverse rigid-limit dipole−dipole coupling of around 30 kHz progressively average the latter, leading to a much larger τ, as is found for the matrix polymer. A dynamic interphase, that naturally arises from a T_g gradient and that was detected in previous work,[13,25,37] is here for sensitivity reasons subsumed in the mobile component. NMR thus detects an apparent minimum fraction of immobilized material with a modulus that is considerably higher than that of the matrix. While the actual SBR contribution to a_{rig} cannot be estimated on the basis of our low-resolution data, it is important to note that other components such as directly surface-bound silane were found to exhibit nearly temperature-independent spectroscopic signatures.[25,38] Note also that the pure matrix SBR shows no detectable a_{rig} (see Figure 4a).

The apparent immobilized fractions a_{rig} are plotted in Figure 4b and are seen to decrease significantly with temperature, as expected for a gradually softening component with activated segmental mobility in combination with a T_g distribution/gradient.[13] It should be stressed that the observed decrease is fully reversible, which excludes significant contributions from evaporating surface water. The observed immobilized fractions are thus distinguished from strongly bound species residing on or in the silica particles that remain immobile up to much higher temperature or from (micro)crystalline wax species that would melt abruptly. The open symbols are data rescaled to ϕ_{silica} = 0.213 assuming a linear dependence of the rigid polymer fraction on the respective silica content of the composite. The data are similar at 25 °C, proving their direct relation to the silica, but are significantly lower at all higher temperatures. Thus, the apparent immobilized fraction is, at higher temperature, increasing more than linearly with ϕ_{silica}, i.e., with the inner surface. This strongly suggests specific nonlinear geometric (surface-to-volume ratio related) confinement effects as the origin, as extensively studied in supported thin-film samples.[14,39]

The second central result is plotted in Figure 5a, where we demonstrate the frequency- and temperature-dependent response of the filler network in terms of ΔG of the highest-filled sample vs temperature for different frequencies ω. The

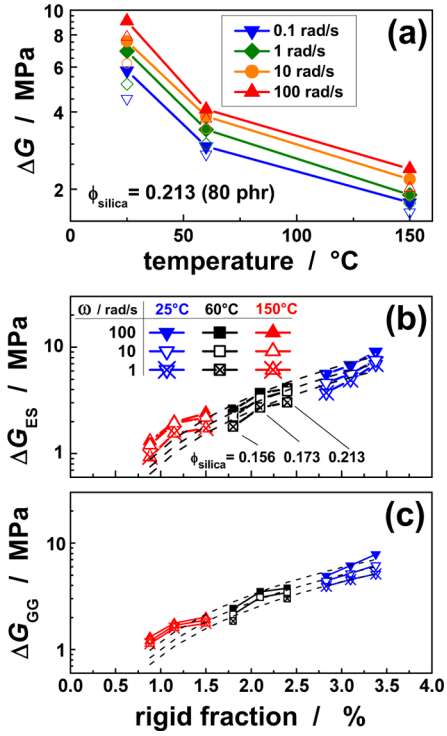

Figure 5. Filler network contribution ΔG to the storage moduli of the composites for different indicated frequencies as a function of (a) temperature and (b,c) NMR-determined rigid component fractions, based upon the (b) ES and (c) GG extrapolations, all plotted semilogarithmically. The solid and open symbols in (a) are based upon ES and GG extrapolations, respectively. The solid lines in (b,c) connect points from samples with ϕ_{silica} = 0.156, 0.173, and 0.213. The dashed lines represent joint fits with independent prefactors for each frequency to power laws, $\Delta G = \Delta G_0(\omega)\phi_{rig}^{\nu}$, with exponents of ν = 1.65 ± 0.11 and 1.46 ± 0.07 for the ES- and GG-based data in (b) and (c), respectively.

dx.doi.org/10.1021/mz500192r | ACS Macro Lett. 2014, 3, 481−485

observation that ΔG decreases monotonically with temperature as well as frequency is in support of the relaxatory, viscoelastic nature of the filler network. The plot also demonstrates that the main conclusions of this work do not depend on whether the ES or the GG model is used for extrapolation and thus ΔG determination (the absolute values of ΔG are slightly lower for the latter).

To establish its connection to the apparent immobilized fraction a_{rig}, Figures 5b/c show ES- and GG-based ΔG values depending on a_{rig} for different frequencies and temperatures for $\phi_{silica} > \phi_c$. We make the surprising observation that ΔG from samples with different ϕ_{silica} measured at different temperatures follows nearly the same strongly nonlinear trends for all frequencies. In other words, we deduce an apparent rigid fraction−temperature superposition property of $\Delta G(\phi_{rig}(T),T)$. A frequency variation leads to a mere overall change by a constant factor, as expected when $\Delta G \sim \omega^{\mu}$ in the investigated range (see Figure 2a).

Since lower values of ΔG are in particular subject to systematic errors related to ambiguities in its determination, it is not possible to make definite conclusions on the functional dependence. A power-law fit appears justified in view of percolation theories and the partially scale-invariant structure of the filler network.[32,36] It should be stressed that a_{rig} quantifies filler-related organic material that above the percolation threshold has a dual function; i.e., it contributes to the bending modulus of the percolated network (see inset of Figure 3b) and is part of rigid agglomerates that shield occluded rubber, thus contributing to hydrodynamic reinforcement. The agglomerates can be, but are not necessarily, part of the percolated filler network.

Concluding our observations, we have demonstrated unambiguous proof of the viscoelastic, relaxatory nature of the filler network contribution ΔG to the elasticity of silica-filled industrial rubber and for the first time revealed a direct correlation with an NMR-detected apparent fraction of immobilized components. The NMR observable quantifies the mechanically most rigid polymer or organic additive components with α relaxation times of 10 μs and above, which for a rubber material far above its bulk T_g ($\tau_\alpha \sim$ ns) must correspond to surface-related slowed-down species. Their fraction is observed to decrease with temperature, as expected for an interphase characterized by a T_g gradient. This explains why a lower temperature leads to a higher bending rigidity of the viscoelastic filler−filler connections and thus to an overall higher ΔG.

AUTHOR INFORMATION

Corresponding Author

*E-mail: kay.saalwaechter@physik.uni-halle.de.

Notes

The authors declare no competing financial interest.

ACKNOWLEDGMENTS

We thank Dr. Sven Thiele (Styron Deutschland GmbH) for providing the SBR, Manfred Klüppel for discussions and valuable suggestions, and the state of Saxony-Anhalt ("Innovationscluster Polymertechnologie I") as well as the Deutsche Forschungsgemeinschaft (DFG), projects SA 982/6-1 (KS) and BE 2352/4-1 (MB) for financial support.

REFERENCES

(1) Medalia, A. *Rubber Chem. Technol.* **1978**, *51*, 437.
(2) Vilgis, T.; Heinrich, G. *Macromolecules* **1994**, *27*, 7846.
(3) Klüppel, M.; Schuster, R. H.; Heinrich, G. *Rubber Chem. Technol.* **1997**, *70*, 243.
(4) Wang, M. J. *Rubber Chem. Technol.* **1998**, *71*, 520.
(5) Leblanc, J. L. *Prog. Polym. Sci.* **2002**, *27*, 627.
(6) Kohls, D.; Beaucage, G. *Curr. Opin. Solid State Mater. Sci.* **2002**, *6*, 183.
(7) Merabia, S.; Sotta, P.; Long, D. R. *Macromolecules* **2008**, *41*, 8252.
(8) Einstein, A. *Ann. Phys.* **1906**, 289−306.
(9) Guth, E.; Gold, O. *Phys. Rev.* **1938**, *53*, 322.
(10) Smallwood, H. M. *J. Appl. Phys.* **1944**, *15*, 758.
(11) Christensen, R. *Mechanics of composite materials*; Wiley: New York, 1979.
(12) Heinrich, G.; Klüppel, M.; Vilgis, T. A. *Curr. Opin. Solid State Mater. Sci.* **2002**, *6*, 195.
(13) Papon, A.; Montes, H.; Hanafi, M.; Lequeux, F.; Guy, L.; Saalwächter, K. *Phys. Rev. Lett.* **2012**, *108*, 065702.
(14) Napolitano, S.; Capponi, S.; Vanroy, B. *Eur. Phys. J. E* **2013**, *36*, 61.
(15) Tsagaropoulos, G.; Eisenberg, A. *Macromolecules* **1995**, *28*, 396.
(16) Donth, E. *J. Polym. Sci. B, Polym. Phys.* **1996**, *34*, 2881.
(17) Berriot, J.; Montes, H.; Lequeux, F.; Long, D.; Sotta, P. *Macromolecules* **2002**, *35*, 9756.
(18) Gusev, A. A. *Macromolecules* **2006**, *39*, 5960.
(19) Long, D.; Sotta, P. *Rheol. Acta* **2007**, *46*, 1029.
(20) Klüppel, M. *J. Phys.: Condens. Matter* **2009**, *21*, 35104.
(21) Wurm, A.; Ismail, M.; Kretzschmar, B.; Pospiech, D.; Schick, C. *Macromolecules* **2010**, *43*, 1480.
(22) Morozov, I.; Lauke, B.; Heinrich, G. *Comput. Mater. Sci.* **2010**, *47*, 817.
(23) Fritzsche, J.; Klüppel, M. *J. Phys.: Condens. Matter* **2011**, *23*, 035104.
(24) Fragiadakis, D.; Bokobza, L.; Pissis, P. *Polymer* **2011**, *52*, 3175.
(25) Papon, A.; Saalwächter, K.; Schäler, K.; Guy, L.; Lequeux, F.; Montes, H. *Macromolecules* **2011**, *44*, 913.
(26) Papon, A.; Montes, H.; Lequeux, F.; Oberdisse, J.; Saalwächter, K.; Guy, L. *Soft Matter* **2012**, *8*, 4090.
(27) Robertson, C.; Lin, C.; Bogoslovov, R.; Rackaitis, M.; Sadhukhan, P.; Quinn, J.; Roland, C. *Rubber Chem. Technol.* **2011**, *84*, 507.
(28) Robertson, C. G.; Rackaitis, M. *Macromolecules* **2011**, *44*, 1177.
(29) Montes, H.; Lequeux, F.; Berriot, J. *Macromolecules* **2003**, *36*, 8107.
(30) Glomann, T.; Schneider, G. J.; Allgaier, J.; Radulescu, A.; Lohstroh, W.; Farago, B.; Richter, D. *Phys. Rev. Lett.* **2013**, *110*, 178001.
(31) Mujtaba, A.; Keller, M.; Ilisch, S.; Radusch, H.; Thurn-Albrecht, T.; Saalwächter, K.; Beiner, M. *Macromolecules* **2012**, *45*, 6504.
(32) Baeza, G. P.; Genix, A.-C.; Degrandcourt, C.; Petitjean, L.; Gummel, J.; Couty, M.; Oberdisse, J. *Macromolecules* **2013**, *46*, 317.
(33) Lorenz, B.; Pyckhout-Hintzen, W.; Persson, B. N. J. *Polymer* **2014**, DOI: 10.1016/j.polymer.2013.12.033.
(34) Payne, A. R. *J. Appl. Polym. Sci.* **1962**, *6*, 57.
(35) Kraus, G. *J. Appl. Polym. Sci.: Appl. Polym. Symp.* **1984**, *39*, 75.
(36) Kantor, Y.; Webman, I. *Phys. Rev. Lett.* **1984**, *52*, 1891.
(37) Kim, S. Y.; Meyer, H. W.; Saalwächter, K.; Zukoski, C. *Macromolecules* **2012**, *45*, 4225.
(38) Saalwächter, K.; Krause, M.; Gronski, W. *Chem. Mater.* **2004**, *16*, 4071.
(39) Rotella, C.; Wübbenhorst, M.; Napolitano, S. *Soft Matter* **2011**, *7*, 5260.